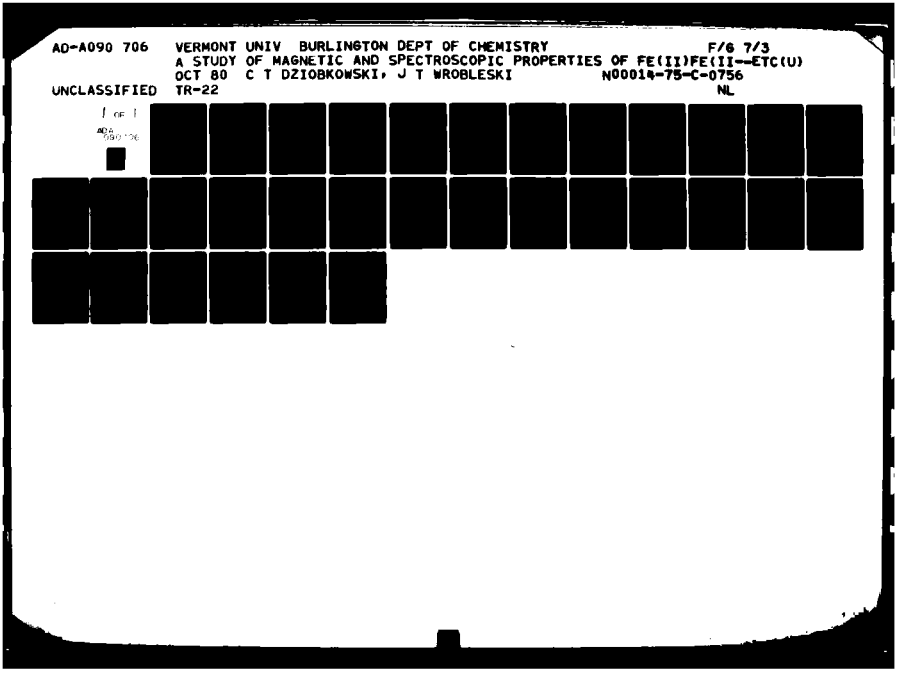
AD-A090 706
VERMONT UNIV BURLINGTON DEPT OF CHEMISTRY F/G 7/3
A STUDY OF MAGNETIC AND SPECTROSCOPIC PROPERTIES OF FE(II)FE(II--ETC(U)
OCT 80 C T DZIOBKOWSKI, J T WROBLESKI N00014-75-C-0756
UNCLASSIFIED TR-22 NL
1 OF 1
AD A090706

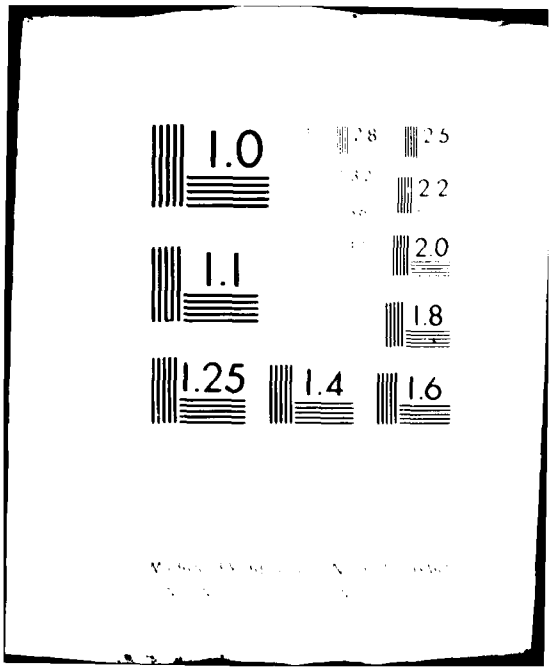
1.0
1.1
1.25
1.4
1.6
1.8
2.0
2.2
2.5

II (12)

OFFICE OF NAVAL RESEARCH

Contract N00014-75-C-0756

Task No. NR 356-593

TECHNICAL REPORT NO. 22

A Study of Magnetic and Spectroscopic Properties of $Fe(II)Fe(III)_2O(CH_3CO_2)_6L_3$, $L = H_2O$ or C_5H_5N. Direct Observation of the Thermal Barrier to Electron Transfer in a Mixed-Valence Complex

by

Chester T. Dziobkowski, James T. Wrobleski and
David B. Brown*

Prepared for publication

in

Inorganic Chemistry

University of Vermont
Department of Chemistry
Burlington, Vermont 05405

October 1, 1980

(14) TR-22

SECURITY CLASSIFICATION OF THIS PAGE (When Data Entered)

REPORT DOCUMENTATION PAGE	READ INSTRUCTIONS BEFORE COMPLETING FORM
1. REPORT NUMBER 22 (6)	2. GOVT ACCESSION NO. AD-A090706 (9)	3. RECIPIENT'S CATALOG NUMBER
4. TITLE (and Subtitle) A Study of Magnetic and Spectroscopic Properties of $Fe(II)Fe(III)_2O(CH_3CO_2)_6L_3$, L=$H_2O$ or C_5H_5N. Direct Observation of the Thermal Barrier to Electron Transfer in a Mixed-Valence Complex*	5. TYPE OF REPORT & PERIOD COVERED Technical Report (5)
	6. PERFORMING ORG. REPORT NUMBER (15)
7. AUTHOR(s) (10) Chester T. Dziobkowski, James T. Wrobleski and David B. Brown*	8. CONTRACT OR GRANT NUMBER(s) N00014-75-C-0756
9. PERFORMING ORGANIZATION NAME AND ADDRESS Department of Chemistry University of Vermont Burlington, Vermont 05405	10. PROGRAM ELEMENT, PROJECT, TASK AREA & WORK UNIT NUMBERS
11. CONTROLLING OFFICE NAME AND ADDRESS Office of Naval Research Department of the Navy Arlington, Virginia 22217 (11) 1	12. REPORT DATE October [illegible]80
	13. NUMBER OF PAGES 27
14. MONITORING AGENCY NAME & ADDRESS(if different from Controlling Office) (12) 32	15. SECURITY CLASS. (of this report) Unclassified
	15a. DECLASSIFICATION/DOWNGRADING SCHEDULE

16. DISTRIBUTION STATEMENT (of this Report)

This document has been approved for public release and sale; its distribution is unlimited.

17. DISTRIBUTION STATEMENT (of the abstract entered in Block 20, if different from Report)

18. SUPPLEMENTARY NOTES

Accepted for publication in Inorganic Chemistry

19. KEY WORDS (Continue on reverse side if necessary and identify by block number)

Mixed-valence, iron acetates, magnetic susceptibility, magnetic exchange, Mössbauer spectroscopy, intervalence transfer, activation energy, electronic relaxation

20. ABSTRACT (Continue on reverse side if necessary and identify by block number)

The mixed-valence iron(II,III,III) acetates, $[Fe_3O(CH_3CO_2)_6L_3]$, where L= water or pyridine, have been prepared and studied by Mössbauer, infrared, and optical spectroscopy and magnetic susceptibility methods. Variable-temperature magnetic susceptibility data for the aquo complex are interpreted on the basis of HDVV $\underline{S}_2 = 2$, $\underline{S}_1 = \underline{S}_3 = 5/2$ spin exchange model with $\underline{J}_{12} = \underline{J}_{23} = -50.0\ cm^{-1}$ and $\underline{J}_{13} = -14.5\ cm^{-1}$. An intervalence transfer band is observed at $13800\ cm^{-1}$

1/-50 cm

1/-14.5 cm

1/13800 cm

405892

20. Abstract

in the room temperature electronic spectrum of the aquo complex. Mössbauer spectra of these compounds are markedly temperature dependent. At 17K absorptions due to distinct Fe(II) and Fe(III) sites are observed while at 300 K a single absorption is observed. Spectra at intermediate temperatures are modeled by assuming intratrimer electronic relaxation between pairs of iron ions. The activation energy for relaxation derived from this model is 470 cm^{-1} for the aquo complex. This energy is equal to the barrier to intramolecular, intervalance thermal electron transfer.

1/2170 cm

A

Introduction

Many transition metal ions form carboxylate complexes which have the basic iron acetate structure.[1] These complexes, of general formula $[M_3O(RCOO)_6L_3]^{n+}$, where L is a neutral, monodentate ligand, contain a triply-bridging oxide ion at the center of a (generally equilateral) triangular array of metal ions. The electronic and structural properties of many of these compounds with M^{3+} (n=1) have been studied. By contrast, few mixed-valence complexes with this structure have been studied in detail. Of these, $Ru_3O(CH_3CO_2)_6(PPh_3)_3$ and $Mn_3O(CH_3CO_2)_6(C_5H_5N)_3$, which formally contain $Ru^{2.67+}$ and $Mn^{2.67+}$, have been examined by single-crystal x-ray crystallography[2,9] and both were found to contain equivalent metal ions. This structural equivalence suggests that complete electron delocalization occurs within the M_3O framework. In addition, ESCA measurements are consistent with complete electron delocalization in several similar ruthenium clusters.[4]

Although these experiments suggest that these materials are Robin and Day[5] Class III-A compounds, it has not been possible to distinguish between complete delocalization (Class III-A) and thermally activated charge transfer (Class II) in the Ru and Mn compounds. By contrast, the mixed-valence iron(II,III,III) acetates,[6] $[Fe_3O(CH_3CO_2)_6L_3]$, where L = H_2O or C_5H_5N, are complexes in which the dynamics of electron transfer may be directly probed by variable-temperature ^{57}Fe Mössbauer spectroscopy. These complexes have been studied by Lupu and co-workers[7-10] who have shown that they are Class II mixed-valence systems, because both iron(II) and iron(III) quadrupole doublets were observed in their low-temperature Mössbauer spectra. However, at room temperature only a single Mössbauer absorption was observed suggesting that thermal electron transfer was fast on the time scale of the Mössbauer experiment (10^{-8}s). Because the experiments of Lupu were carried out over a limited temperature range, and becuase no detailed interpretation of the resulting spectral changes was advanced, we have re-examined these compounds. The temperature dependence of the Mössbauer spectrum of this complex, which

we report here, provides a unique opportunity to obtain information on the energetics and dynamics of electron-transfer in a mixed-valence complex.

Experimental Section

All chemicals used were reagent grade unless specified. Pyridine was dried by refluxing with solid NaOH and purified by fractional distillation.

Preparation of Complexes

$[Fe(II)Fe(III)_2O(CH_3COO)_6(H_2O)_3]$. μ_3-Oxo-triaquohexakis(acetato)iron(II)diiron (III) was prepared according to a modification of the method of Chretien and Lous.[6] A solution of 60 g (0.30 mole) of $FeCl_2 \cdot 4H_2O$ in 200 mL of water was placed in a 2000 mL round bottom flask. A suspension of 111.4 g (0.63 mole) of $Ca(CH_3CO_2)_2 \cdot H_2O$ in 178 mL of H_2O and 378 mL (6.3 moles) of concentrated acetic acid were added. The reaction mixture was continuously aerated, heated to 70°C and maintained at that temperature for six hours. A reflux condenser kept evaporation to a minimum. The mixture was cooled to room temperature and the black crystalline precipitate collected by centrifugation. The product was washed twice with 50 mL of 0.083 M acetic acid, centrifuged and dried under high vacuum. The product was stored in a sealed vial under nitrogen in a desiccator filled with nitrogen; yield 41.7g (69.1%) Anal. Calcd for $C_{12}Fe_3H_{24}O_{16}$: C, 24.35; Fe, 28.31; H, 4.09. Found: C, 24.16; Fe, 27.90; H, 4.14.

$[Fe(II)Fe(III)_2O(CH_3COO)_6(C_5H_5N)_3](C_5H_5N)_{0.5}$ μ_3-Oxo-trispyridinehexakis(acetato) iron(II)diiron(III)hemipyridine was prepared according to a modification of the method of Lupu and Ripan.[8] $[Fe(II)Fe(III)_2O(CH_3COO)_6(H_2O)_3]$(8.5g, 0.0144 mole) was mixed with 50 mL of pyridine which had been saturated with nitrogen gas in a nitrogen atmosphere. After twenty minutes of constant stirring, the black crystalline product was collected by filtration and dried under high vacuum. The product was stored in a sealed vial under nitrogen in a desiccator filled with nitrogen; yield 6.45g (55.1%). Anal. Calcd for $C_{29.5}Fe_3H_{35.5}N_{3.5}O_{13}$; C, 43.49; Fe, 20.57; H, 4.39; N, 6.02. Found: C, 43.13; Fe, 20.55;

H, 4.24; N, 6.06.

Physical Measurements. Magnetic susceptibilities, elemental analyses, Mössbauer spectra and calculations were performed as described in the preceding work.[11] Mössbauer spectra were deconvoluted to a sum of Lorentzian absorptions plus parabolic baseline with a program described by Lang and Dale.[12] Electronic spectra were obtained on a Cary 14 spectrophotometer with samples dispersed in Fluorolube grease (GR-90 , Hooker Chemical Company), between quartz plates or dispersed in thin films of polystyrene.

Results and Discussion

Magnetic Susceptibilities. Although to date no complete crystal structure has been reported for either the mixed-valence acetate aquo complex or its pyridine adduct, the pyridine adduct has been reported to be isostructural with the manganese analog.[3] Because the manganese complex contains an equilateral triangle of metal ions, it is probable that this geometry holds for the aquo, as well as the pyridine, iron complex. However, as shown by the Mössbauer spectra (vide infra), on some time scale the iron sites are electronically distinguishable. Consequently the system may be treated in the Heisenberg-Dirac-Van Vleck (HDVV) formalism as an $\underline{S}_2=2, \underline{S}_1=\underline{S}_3=5/2$ trimer. As described by Kambe,[13] the appropriate spin Hamiltonian is:

$$\underline{H} = -2\underline{J}(\underline{S}_1\cdot\underline{S}_2 + \underline{S}_2\cdot\underline{S}_3) - \underline{J}'(\underline{S}_1\cdot\underline{S}_3), \qquad (1)$$

where

$\underline{J}$ = Fe(II)-Fe(III) exchange parameter

$\underline{J}'$ = Fe(III)-Fe(III) exchange parameter

$\underline{S}_i$ = spin on the individual ion ($\underline{S}_1, \underline{S}_2$: Fe(III); $\underline{S}_2$: Fe(II)).

The expression for the energy (eq 2) of each spin state can be derived in the normal manner.[14]

$$\underline{E}(\underline{S}^*,\underline{S}') = \frac{2\underline{Z}\underline{J}}{\underline{n}-1}[\underline{S}'(\underline{S}'+1) - \underline{S}^*(\underline{S}^*+1)] - \frac{\underline{Z}\underline{J}'}{\underline{n}-1}[\underline{S}^*(\underline{S}^*+1)] \qquad (2)$$

where

$\underline{E}(\underline{S}^*,\underline{S}')$ = energy of a spin state

$\underline{Z}$ = number of nearest neighbors (=2)

$\underline{n}$ = number of interacting paramagnetic ions (=3)

$\underline{S}^* = \underline{S}_1+\underline{S}_3, \underline{S}_1+\underline{S}_3-1, \ldots\ldots\ldots\ldots, 0$

$\underline{S}' = \underline{S}^*+\underline{S}_2, \underline{S}^*+\underline{S}_2-1, \ldots\ldots\ldots\ldots, 0$

When the energies are substituted into the appropriate molar susceptibility partition function[14], the result is the working expression for the theoretical molar susceptibility, eq 3. We have included this equation because it disagrees, in several terms, with that which has previously been reported by Lupu.[7]

Lupu[7] measured the susceptibility of the aquo complex over the range of 94-296 K. Exchange parameters were obtained by finding the best fit of the experimental susceptibility to the (incorrect) theoretical expression at a single temperature. This procedure, repeated at two other temperatures, led to exchange parameters which were themselves temperature dependent; that is, the values of $\underline{J}$ ranged from +2.8 cm^{-1} at 101 K to -10 cm^{-1} at 288 K. We have measured the susceptibility over the range 17-294 K. The data are given in Table I[15] and shown graphically in Figure 1. Over the coincident temperature range, the data are in excellent agreement with those reported by Lupu. The data have been fit to eq 3 by employing the Simplex minimization algoritm.[16,17] The best fit, assuming $\underline{g}$ = 2.00, is shown as the solid curve in Figure 1. The calculated values of the exchange parameters are $\underline{J}$ = -50.0 and $\underline{J}'$ = -14.5 cm^{-1} ($\underline{J}/\underline{J}'$ = 3.47). Although a direct comparison of exchange parameters in similar iron(III) compounds is difficult to make these values have an average near that of for example, $[Fe_3O(CH_3CO_2)_6(H_2O)_3]ClO_4$.[11] The success of eq 3 at describing the susceptibility of the aquo complex suggests that it, like the pyridine complex, does adopt the basic iron acetate structure.

The relatively much stronger Fe(II)-Fe(III) exchange integral reflects in part the greater number of pathways available for this exchange. Its larger value is, moreover, consistent with the Mössbauer results (vide infra) which demonstrate that electronic

$$\bar{\chi}_M = \frac{N\beta^2 g^2}{3kT}\,\frac{\left[\begin{array}{llll}
840\exp(-26X-30Y) & +546\exp(-12X-30Y) & +330\exp(-30Y) & \\
+180\exp(10X-30Y) & +84\exp(18X-30Y) & +546\exp(-22X-20Y) & \\
+330\exp(-10X-20Y) & +180\exp(-20Y) & +84\exp(8X-20Y) & \\
+30\exp(14X-20Y) & +330\exp(-18X-12Y) & +180\exp(-8X-12Y) & \\
+84\exp(-12Y) & +30\exp(6X-12Y) & +6\exp(10X-12Y) & \\
+180\exp(-14X-6Y) & +84\exp(-6X-6Y) & +30\exp(-6Y) & \\
+6\exp(4X-6Y) & & +84\exp(-10X-2Y) & \\
+30\exp(-4X-2Y) & +6\exp(-2Y) & +30\exp(-6X) &
\end{array}\right]}{\left[\begin{array}{llll}
15\exp(-26X-30Y) & +13\exp(-12X-30Y) & +11\exp(-30Y) & \\
+9\exp(10X-30Y) & +7\exp(18X-30Y) & +13\exp(-22X-20Y) & \\
+11\exp(-10X-20Y) & +9\exp(-20Y) & +7\exp(8X-20Y) & \\
+5\exp(14X-20Y) & +11\exp(-18X-12Y) & +9\exp(-8X-12Y) & \\
+7\exp(-12Y) & +5\exp(6X-12Y) & +3\exp(10X-12Y) & \\
+9\exp(-14X-6Y) & +7\exp(-6X-6Y) & +5\exp(-6Y) & \\
+3\exp(4X-6Y) & +1\exp(6X-6Y) & +7\exp(-10X-2Y) & \\
+5\exp(-4X-2Y) & +3\exp(-2Y) & +5\exp(-6X) &
\end{array}\right]}, \qquad (3)$$

where $X = J/kT$ and $Y = J'/kT$.

relaxation between Fe(II) and Fe(III) sites is much more facile than that between Fe(III) and Fe(III) sites.

The pyridine complex has a temperature-dependent susceptibility which is similar to the aquo complex. The data, and best fit to eq 3, are shown in Figure 2 and detailed in Table II.[15] The exchange parameters, $J = -37.2$ and $J' = -11.2$ cm^{-1} are somewhat larger than in the aquo complex, whereas the ratio $J/J' = 3.32$ is similar to that of the aquo complex.

Mössbauer Spectra

Aquo Complex. Representative variable-temperature (17-298 K) Mössbauer spectra of the mixed-valence aquo complex are illustrated in Figure 3. At 17 K the spectrum consists of three clearly resolved absorptions. As the temperature is increased the resonant absorptions coalesce and the apparent intensity of the high velocity line decreases. The final spectrum at 298 K has the appearance of a single broadened absorption centered at approximately 0.75 mm/s. These changes are reversible provided the sample is not heated above room temperature. At T>298 K we do not observe further narrowing of the Mössbauer absorption but rather a gradual, irreversible oxidation and/or dehydration of the sample occurs and the spectrum broadens as a result of the decomposition. Indeed, prolonged heating of the sample at 373 K in vacuum results in the formation of a spectrum composed of a single quadrupole doublet with $\delta = 0.6$ mm/s and $\Delta = 0.75$ mm/s. After this heat treatment the two line spectrum persists to 17 K.

Although only three absorptions are resolved in the spectra below 200 K, it is obvious from inspection of the relative line intensities that two absorptions are nearly coincident at approximately 0.1 mm/s. The 17 K spectrum was fit to four absorptions with the constraint that one of the absorptions at 0.1 mm/s be equal to the high energy absorption at ca. 2.6 mm/s and that the remaining two absorptions also be equal to one another. The two less intense absorptions were found at 0.190 and 2.589 mm/s whereas the remaining lines with larger intensity were located at 0.028 and 0.984 mm/s. Further-

more, the ratio of the areas of the 0.984 to the 2.589 mm/s absorption was 1.77. On the basis of calculated quadrupole splittings and isomer shifts the absorptions at 0.190 and 2.589 mm/s were assigned to Fe(II) transitions (δ = 1.39 and Δ = 2.40 mm/s) and those at 0.028 and 0.984 mm/s to Fe(III) transitions (δ = 0.51 and Δ = 0.98 mm/s). Although this four-line fit is statistically acceptable ($\underline{R}$=2.3),[18] the area ratio of 1.77 is significantly less than the anticipated value of 2.0. This discrepancy is larger at higher temperatures. Thus, the Fe(III)/Fe(II) area ratio increases to 2.60 at 225 K and ca. 4.0 at 280 K. We do not believe that this variable area ratio results entirely from a difference in the temperature dependence of the recoilless fraction ratio of Fe(III) to Fe(II) sites in this material. Rather, we propose that intramolecular Fe(II) $\longrightarrow$ Fe(III) thermal electron transfer is responsible for the observed temperature dependent Mössbauer spectra (vide infra).

In order to theoretically model the Mössbauer spectra shown in Fig. 3, we adopted the relaxation model which is illustrated in Fig. 4. The spectral transitions, ω_i, are given in units of mm/s in Fig. 4. The mathematical formalism which was applied to this relaxation model is based on the quantum mechanical density matrix equations of motion $\underline{dG_i/dt}$ given by Wickman.[19] Details of the mathematics will not be given here. However, it is important to briefly sketch the important computational features of the model. Theoretical Mössbauer spectra were calculated from the known solution to the equations of motion, which is, in this instance, expressed by eq 4.

$$\underline{I_2}(\omega) = \sum^{1}[(1+\tau_{\underline{i}}\Gamma_{\underline{i}})\underline{P_i} + \underline{Q_i}\underline{R_i}]/(P_i^2 + R_i^2) \qquad (4)$$

In eq 4 the subscript $\underline{i}$ refers to an individual Mössbauer transition and $\underline{P_i}$ = $\tau_{\underline{i}}[\Gamma_{\underline{i}}^2 - (\Delta_{\underline{i}}' - \omega)^2 + \delta_{\underline{i}}'^2] + \Gamma_{\underline{i}}$, $\underline{R_i} = (\Delta_2' - \omega)(1 + 2\tau_{\underline{i}}\Gamma_{\underline{i}})$, $\underline{Q_i} = \tau_{\underline{i}}(\Delta_{\underline{i}}' - \omega)$, and $\Gamma_{\underline{i}}$ is the linewidth for transition $\underline{i}$. In our model, relaxation processes occur between Fe^{2+} and Fe^{3+} nuclear energy levels ($3+ \leftrightarrow 2+$) and also between pairs of Fe^{3+} nuclear

energy levels (3+ ↔ 3+). It is therefore necessary to compute the Mössbauer spectrum for six transition frequencies which enter eq 4 through the Δ_i' and δ_i' terms given in eq 5. The model was constructed with equal probability for all transitions. Furthermore the 3+ ↔ 3+ relaxation time was assumed to be much longer than the nuclear excited

$$\begin{aligned}
\Delta_1' &= \tfrac{1}{2}(\omega_1+\omega_3) & \delta_1' &= \tfrac{1}{2}(\omega_1-\omega_3) \\
\Delta_2' &= \tfrac{1}{2}(\omega_2+\omega_4) & \delta_2' &= \tfrac{1}{2}(\omega_2-\omega_4) \\
\Delta_3' &= \Delta_2' & \delta_3' &= \tfrac{1}{2}(\omega_4-\omega_2) \\
\Delta_4' &= \Delta_1' & \delta_4' &= \tfrac{1}{2}(\omega_3-\omega_1) \\
\Delta_5' &= \omega_1 & \delta_5' &= \delta_6' = 0 \\
\Delta_6' &= \omega_2
\end{aligned} \qquad (5)$$

state lifetime (99.7 ns) and was arbitrarily set at 200 ns. Arbitrarily longer 3+ ↔ 3+ relaxation times had no obvious effect on the calculated spectra. The linewidth for 2+ ↔ 3+ transitions was assumed to be equal to the natural linewidth (0.1946 mm/s) whereas the 3+ ↔ 3+ linewidth was empirically determined to be 0.30 ± 0.05 mm/s and therefore was set at 0.30 mm/s for all calculations.

In fitting the experimental spectra to this model the Fe^{2+} and Fe^{3+} isomer shifts and quadrupole splittings were parameterized as well as the 2+ ↔ 3+ relaxation time. Computer minimization of eq 4 resulted in the theoretical spectra illustrated as smooth curves in Fig. 3. "Best fit" values of δFe(II), δFe(III), ΔFe(II), ΔFe(III), and τ(2+ ↔ 3+) are given in Table III. Values of τ(2+ ↔ 3+) calculated in this manner are presented as an Arrhenius activation energy plot in Fig.5. In this figure the open circles refer to relaxation times which were obtained by direct minimization in the manner previously outlined. The range of relaxation time values at each temperature, represented by lines parallel to the -log(1/τ) axis, is intended to illustrate the relative uncertainty in τ according to this model. These "uncertainty bars" were obtained by holding δFe(II), δFe(III), ΔFe(II), and ΔFe(III) constant and changing τ(2+ ↔ 3+) until the sum

of squares was doubled. In some instances, particularly at the low and high temperature limits, the calculated spectra are quite insensitive to variations in $\tau(2+ \leftrightarrow 3+)$. However at intermediate relation times the spectra are quite sensitive to rather small ($\sim$2 ns) changes in τ. In order to extract an energy barrier from these data, the open circle points were least-squares fit to a straight line. The result of this fit is illustrated as the line in Fig. 5. The slope of this line is 303 K. By employing the relation $\underline{E} = 2.303\ \underline{k_B} \cdot \text{slope}$, where $\underline{k_B}$ is Boltzmann's constant, we obtain an activation energy of 470 cm^{-1}. Because of the definition of $\tau(2+ \leftrightarrow 3+)$ in this model, $\underline{E}$ may be interpreted as the thermal barrier to electron transfer in this mixed-valence trimer. The magnitude of this barrier has a rather large uncertainty, as it is obvious that the fit of Figure 5 is not unique. Furthermore, non-Arrhenius behavior may be more appropriate in this case.[20] However, because the data at the high and low temperature extremes are so insensitive to the choice of τ, we do not believe that the use of more complicated, non-linear, fits to the data are justified.

Fig. 6 illustrates the temperature dependence of the isomer shift of the Fe(II) and Fe(III) sites, shown as open and filled circles, respectively. Because these isomer shifts are not corrected for second-order Doppler shift effects, it appears that the Fe(II) isomer shift is decreasing at a much greater rate than the Fe(III) isomer shift is increasing. In the absence of second-order Doppler effects, the isomer shifts are seen to converge at approximately 350 K. The second-order Doppler effect may be visualized by plotting the average of the Fe(II) and Fe(III) isomer shifts. These average δ values are shown as half-filled circles in Fig. 6. The straight line drawn through these points represents the high-temperature limiting form of the second-order Doppler shift (slope = 6.3×10^{-4} mm/s K^{-1}).

The temperature variation of the quadrupole splitting for both Fe(II) and Fe(III) sites is illustrated in Fig. 7. These quadrupole splittings are apparently converging to approximately 0 mm/s between 320 and 350 K. This averaging of quadrupole splittings to zero is taken account of in the model by assuming that the $|\pm\frac{1}{2}\rangle$ excited nuclear energy level lies above the $|\pm 3/2\rangle$ level (see Fig. 4); that is to say, Δ is negative for the

Fe(II) site in this complex. An average quadrupole splitting of zero in this case is only possible if $\Delta Fe(II)$ and $\Delta Fe(III)$ are of opposite sign.

Pyridine Complex. The gross features of the variable-temperature Mössbauer spectra of the pyridine complex are similar to those of the aquo complex. A number of details of the spectra are different, however. The representative spectra illustrated in Fig. 8 point out some of the differences. Firstly, the pyridine complex possesses a much smaller recoilless fraction than the aquo complex. This smaller $\underline{f}$ value is reflected in the statistically-poorer pyridine spectra. Only very poorly resolved spectra were obtained above 200 K. Because of the poor quality of the high temperature spectra, we were unable to extract meaningful δ, Δ, and τ parameters through application of our relaxation model. At lower temperatures, however, we were able to obtain useful spectral parameters for the relaxation process. These values are listed in Table IV. A plot of $-\log(1/\tau)$ vs $1/\underline{T}$ gives an activation energy of 150 cm^{-1} for the thermal electron transfer barrier in the pyridine complex. This value is however subject to a large uncertainty because of the relative insensitivity of the spectra to rather large changes in $\tau(2+ \leftrightarrow 3+)$. A smaller value of $\underline{E}$ for the pyridine relative to the aquo complex is, nonetheless, indicated by the fact that the Mössbauer spectrum of the pyridine complex shows rapid electron transfer at approximately 200 K whereas this rapid electron transfer is only observed at ca. 300 K in the aquo complex.

Infrared Spectra. Infrared spectra for the mixed valence acetate complexes are shown in Figure 9, and band assignments are listed in Tables V and VI.[15] Vibrations were assigned using the conventions of Nakamoto,[21] and are, for the most part, consistent with the assignments of Grecu and Lupu.[10] Of particular importance is an absorption near 530 cm^{-1} which has been assigned[10] to the asymmetric stretch of the Fe_3O core [$\nu_s(Fe_3O)$]. This same absorption is present in the singly-valent Fe(III) complexes,[22] although Griffith[23] has assigned this mode to an absorption at 588 cm^{-1}. For the local D_{3h} symmetry of the M_3O core, the symmetric stretching mode [$\nu_s(Fe_3O)$] is Raman, but not infrared, active. Although no Raman data have been reported for any of the mixed-

valence complexes, Griffith[23] has assigned a Raman band at 181 cm^{-1} in the Fe(III) complex to this absorption.

Electronic Spectra. Figure 10 shows the room temperature electronic spectrum of $Fe_3O(CH_3CO_2)_6(H_2O)_3$. Broad absorptions at 8200 and 9700 cm^{-1} are typical of the $Fe(II)O_6$ chromophore and the singly-valent Fe(III) analog exhibits absorptions in this region as well.[22] We assign the absorption at 13800 cm^{-1}, which is not present in the singly-valent complex, to an intervalence transfer band. Intervalence transfer absorptions have been observed in this region in other single-atom bridged Fe(II,III) complexes,[24] but the lack of resolution of this band precludes detailed analysis.

Conclusions. Data obtained from a variety of physical methods demonstrate that the mixed-valence iron (II,III,III) acetates undergo dynamic intratrimer electron transfer. Using ^{57}Fe Mössbauer spectroscopy, rate constants for the intervalence transfer have been determined. Although the precision is not high, the barriers to thermal electron transfer have been extracted using an Arrhenius activation model. Recent theoretical work[25] has shown that many of the spectral properties of mixed-valence compounds are explicable in terms of a vibronic coupling model. For a symmetrical mixed-valence complex (such as is the case here) thermal intervalence transfer should be a phonon-assisted process in which the ions are coupled by the asymmetric stretching vibrational mode of the interacting ions. It may prove possible to interpret the temperature dependence of the Mössbauer spectra using the vibronic coupling model for the electron transfer process, or using other models which consider tunnelling transitions explicitly. Such interpretations, however, must await more detailed theoretical and experimental examination.

These compounds have provided a unique opportunity to determine directly the energetics of thermal electron transfer. This thermal barrier has been determined in only one other molecule system.[26] Gagne and co-workers have used EPR measurements to estimate the electron-transfer rate, and thus the actuation energy, in a binuclear

copper (I,II) complex. Other compounds, such as the Creutz and Taube (C-T) complex $[(NH_3)_5Ru\text{-pyr-}Ru(NH_3)]^{5+}$ (pyr = pyrazine), exhibit apparent[27] thermally-activated electron transfer, but experimental probes to measure the barrier directly are not available. Thus, although electron transfer is known to be fast at room temperature, on the time scale of ^{99}Ru Mössbauer spectroscopy (ca. 10^{-9} sec) valences are trapped at 4 K.[28] The same types of information which we have obtained for the mixed-valence iron acetate are, in principle, obtainable from temperature-dependent ^{99}Ru Mössbauer spectroscopy. Unfortunately, low recoil-free fractions preclude the observation of ^{99}Ru Mössbauer spectra at temperatures where thermally activated electron transfer is facile.

The thermal barrier to electron transfer has been measured by using Mössbauer spectroscopy in other cases. Using ^{151}Eu Mössbauer spectroscopy, Eu_3S_4 has been shown to undergo intervalence electron hopping with an activation energy of 0.24 eV.[29] Electron hopping in this system, a continuous lattic semiconductor, can be correlated with the activation energy of 0.22 eV determined from electrical conductivity measurements. The semiconductor Sn_2S_3 has also been studied by variable-pressure ^{119}Sn Mössbauer spectroscopy.[30] The results of this study are, however, more consistent with a "valence polarization" rather than true electron transfer in Sn_2S_3. Thus, $Fe_3O(CH_3CO_2)_6(H_2O)_3$ and its pyridine analog provide a unique probe to the dynamics of electron transfer in molecular mixed-valence compounds, and may consequently serve as important systems on which to focus efforts on fundamental understanding of the mixed-valence phenomenon.

Acknowledgement. This work was supported in part by the Office of Naval Research. We thank Dr. E. E. Weltin for helpful discussions.

Supplementary Material Available: Experimental and calculated magnetic susceptibilities, Tables I and II; infrared spectral data and assignments, Tables V and VI. (7 pages). Ordering information is given on any current masthead page.

References and Notes

1. Figgis, B.N.; Robertson, G.B., Nature 1965, 205, 694. Orgel, L.E., Nature 1960, 187, 504.

2. Cotton, F.A., Norman, J.G., Inorg. Chem. Acta 1972, 6, 411.

3. Baikie, A.R.E.; Hursthouse, M.B.; New, D.B.; Thornton, P., J. Chem. Soc. Chem. Comm. 1978, 62.

4. Wilson, S.T.; Bondurant, R.F.; Meyer, T.J.; Salmon, D.J., J. Am. Chem. Soc. 1975, 97, 2285. Baumann, J.A.; Salmon, D.J.; Wilson, S.T.; Meyer, T.J.; Hatfield, W.E., Inorg. Chem. 1978, 17, 3342.

5. Robin, M.B.; Day, P., Adv. Inorg. Chem. Radiochem. 1967, 10, 247.

6. Chretien, A.; Lous, E., Bull. Soc. Chim. Fr. 1944, 11, 446.

7. Lupu, D., Rev. Roum. Chim. 1970, 15, 417.

8. Lupu, D.; Ripan, R., Rev. Roum. Chim. 1971, 16, 43.

9. Lupu, D.; Barb, D.; Filoti, G.; Morariu, M.; Tarina, D., J. Inor. Nucl. Chem. 1972, 34, 2803.

10. Grecu, R.; Lupu, D., Rev. Roum. Chim. 1971, 16, 1811.

11. Dziobkowski, C.T.; Wrobleski, J.T.; Brown, D.B., Inorg. Chem. 1980, 19, 0000. (Previous paper).

12. Lang, G.; Dale, B.W., Nucl. Instrum. Methods 1974, 116, 567.

13. Kambe, K., J. Phys. Soc. Jpn. 1950, 5, 48.

14. Mabbs, F.E., Machin, D.J., "Magnetism and Transition Metal Complexes"; Chapman and Hall; London 1973, pp. 190-196.

15. See Supplementary Material.

16. Deming, S.N.; Morgan, S.L., Anal. Chem. 1973, 45, 278A.

17. Dean, W.K.; Heald, K.J.; Deming, S.N., Science 1975, 189, 805.

18. R is defined as the ratio of the normalized sum of the squares of the residuals to the number of degrees of freedom in the fit.

19. Wickman, H.H., "Mössbauer Effect Methodology", I.J. Gruverman, Ed., Plenum Press, New York, 1966, p. 39.

20. LaPlante, J.-P.; Siebrand, W., Chem. Phys. Lett. 1978, 59, 433.

21. Nakamoto, K., "Infrared Spectra of Inorganic and Coordination Compounds", Wiley, New York 1970.

22. Long, G.J.; Robinson, W.T.; Tappmeyer, W.R.; Bridges, D.L., J. Chem. Soc., Dalton Trans. 1973, 573.

23. Griffith, W.P., J. Chem. Soc. (A) 1969, 2270.

24. Walton, E.G.; Corvan, P.J.; Brown, D.B.; Day, P., Inorg. Chem. 1976, 15, 1737.

25. Piepho, S.B.; Krausz, E.R.; Schatz, P.N., J. Am. Chem. Soc. 1978, 100, 2996. Wong, K.Y.; Schatz, P.N.; Piepho, S.B., J. Am. Chem. Soc. 1979, 101, 2793.

26. Gagné, R.R.; Koval, C.A.; Smith, T.J., Cimolino, M.C., J. Am. Chem. Soc. 1979, 101, 4571.

27. There is some controversy regarding this material, particularly with respect to a trapped vs. delocalized ground state description. Arguments favoring a trapped (Class II) ground state are summarized in Bunker, B.C.; Drago, R.S.; Hendrickson, D.N.; Richman, R.M.; Kessell, S.L., J. Am. Chem. Soc. 1978, 100 3805. Arguments favoring a delocalized (Class III) ground state are detailed in Hush, N.S., "Mixed-Valence Compounds," Brown, D.B., ed., Reidel, Dordrecht, 1980; p. 151.

28. Creutz, C.; Good, M.L.; Chandra, S., Inorg. Nucl. Chem. Lett. 1973, 9, 171.

29. Berkooz, O.; Malamud, M.; Shtrikman, S., Sol. State Comm. 1968, 6, 185.

30. Amthauer, G.; Fenner, J.; Hafner, S.; Holzapfel, W.B.; Keller, R., J. Chem. Phys. 1979, 70, 4837.

Table III. Mössbauer Spectral Data for the Aquo Complex.

T, K	δFe(II), mm/s[a]	δFe(III), mm/s[a]	ΔFe(II), mm/s	ΔFe(III), mm/s	τ, ns
17.0	1.35	0.52	2.52	0.99	>2444.
130.0	1.34	0.50	2.38	0.95	196.
170.0	1.28	0.51	2.28	0.89	116.
200.0	1.24	0.49	2.21	0.83	95.3
210.0	1.20	0.49	2.00	0.79	62.7
225.0	1.19	0.52	1.70	0.74	21.5
235.0	1.14	0.52	1.64	0.72	22.0
245.0	1.15	0.54	1.66	0.72	20.4
260.0	1.14	0.54	1.56	0.68	18.0
280.0	1.06	0.55	1.10	0.58	11.6
298.0	0.99	0.56	0.77	0.24	2.5

[a] Relative to α-Fe.

Table IV. Mössbauer Spectral Data for the Pyridine Complex.

T, K	δFe(II), mm/s[a]	δFe(III), mm/s[a]	ΔFe(II), mm/s	ΔFe(III), mm/s	τ, ns
16.8	1.18	0.56	2.85	1.08	>200.
50.0	1.14	0.55	2.80	1.06	11.5
75.0	1.16	0.55	2.61	1.06	11.7
130.0	1.17	0.52	2.39	1.12	9.7
195.0	1.05	0.51	1.80	1.06	8.0
200.0	0.91	0.50	1.77	1.03	5.4

[a] Relative to α-Fe.

Figure Captions

Fig. 1. Molar magnetic susceptibility and effective magnetic moment vs temperature for $[Fe(II)Fe(III)_2O(CH_3COO)_6(H_2O)_3]$. The solid line gives the theoretical fit to the HDVV model with $\underline{S}_1 = \underline{S}_3 = 5/2$ and $\underline{S}_2 = 2$ with $\underline{J} = -50.0$ cm^{-1}, $\underline{J}' = -14.5$ cm^{-1} and $\underline{g} = 2.00$.

Fig. 2. Molar magnetic susceptibility and effective magnetic moment vs temperature for $[Fe(II)Fe(III)_2O(CH_3COO)_6(C_5H_5N)_3]\ (C_5H_5N)_{0.5}$. The solid line gives the theoretical fit to the HDVV model with $\underline{S}_1 = \underline{S}_3 = 5/2$ and $\underline{S}_2 = 2$ with $\underline{J} = -37.2$ cm^{-1}, $\underline{J}' = -14.5$ cm^{-1} and $\underline{g} = 2.00$.

Fig. 3. Variable-temperature Mössbauer spectra of the aquo complex (9 mgFe/cm^2, sample dispersed in vaseline). The solid lines represent theoretical fits obtained by using the relaxation model described in the text.

Fig. 4. An illustration of the relaxation model employed to calculate Mössbauer spectra for the mixed-valence acetate trimers.

Fig. 5. A plot of $-\log(1/\tau)$ vs $1/T$ for the aquo complex. The "uncertainty bars" are described in the text. The straight line is a least-squares fit to the open circles and results in an activation energy of 470 cm^{-1}.

Fig. 6. A plot of the temperature dependence of derived isomer shifts for the Fe(II) (open circles), Fe(III) (filled circles), and average oxidation state (half filled circles) sites in the aquo complex. The solid line represents the second order Doppler shift correction to the isomer shift of the average oxidation state.

Fig. 7. A plot of the temperature variation of the derived quadrupole splittings of the Fe(II) (open circles) and Fe(III) (filled circles) sites in the aquo complex.

Fig. 8. Representative variable-temperature Mössbauer spectra of the pyridine mixed-valence trimer. The solid lines represent theoretical fits obtained by using the relaxation model described in the text.

Fig. 9 Infrared spectra of the mixed-valence acetate complexes.

Fig. 10 Room temperature electronic spectrum of $Fe_3O(CH_3CO_2)_6(H_2O)_3$.

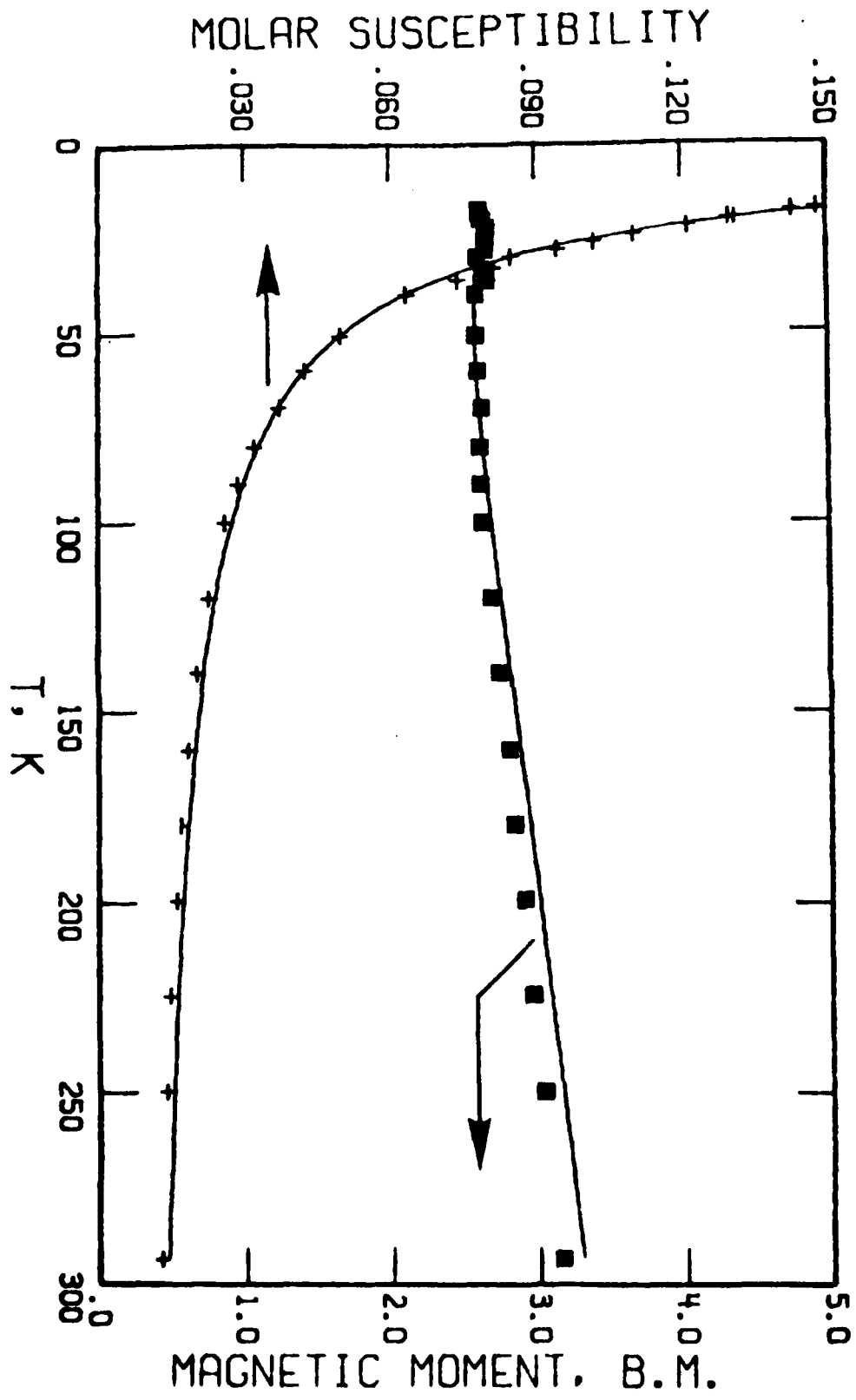
MOLAR SUSCEPTIBILITY
.030
.060
.090
.120
.150
0
50
100
150
200
250
300
T, K
1.0
2.0
3.0
4.0
5.0
MAGNETIC MOMENT, B.M.

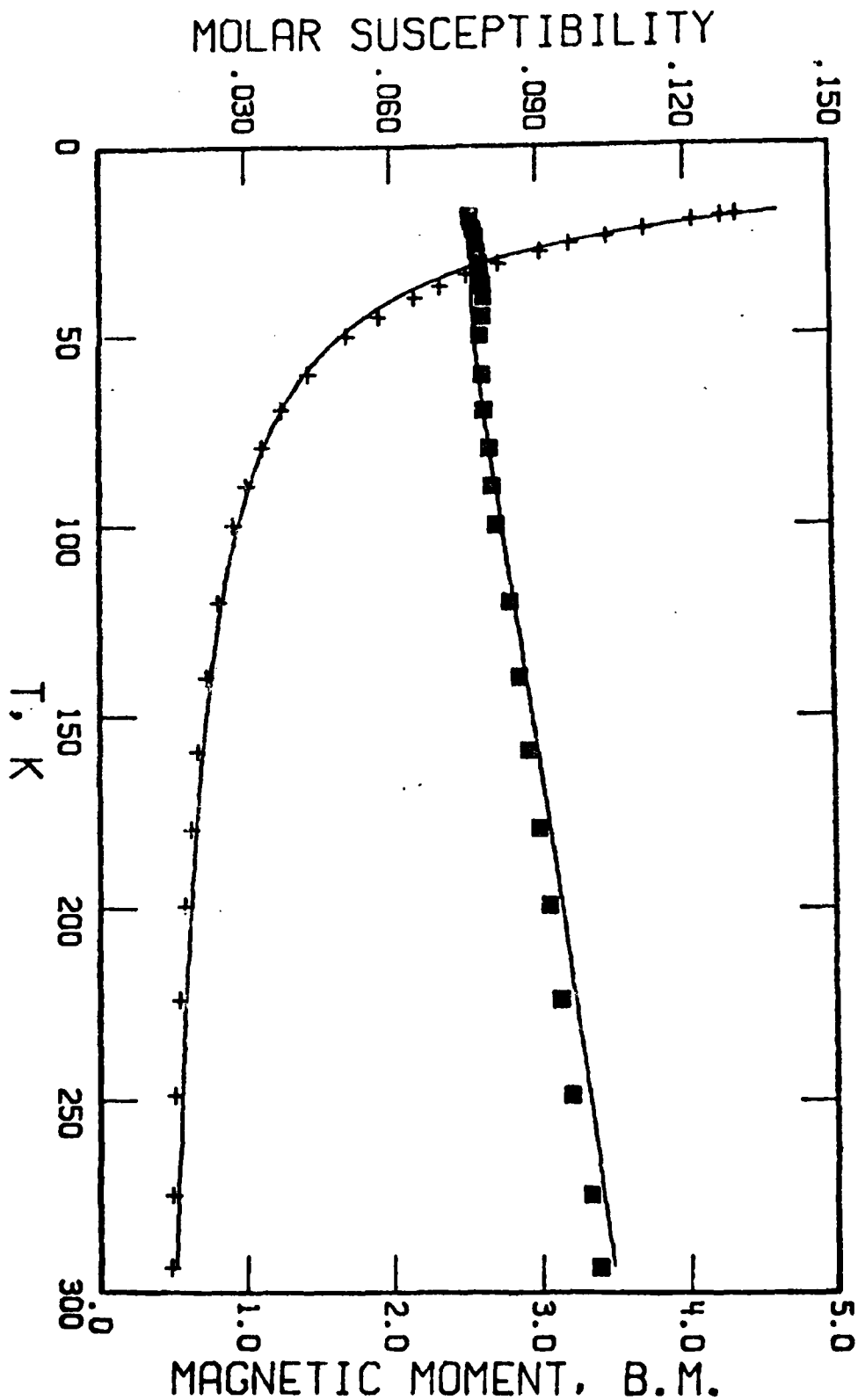
MOLAR SUSCEPTIBILITY
.030
.060
.090
.120
.150
0
50
100
150
200
250
300
T, K
0.0
1.0
2.0
3.0
4.0
5.0
MAGNETIC MOMENT, B.M.

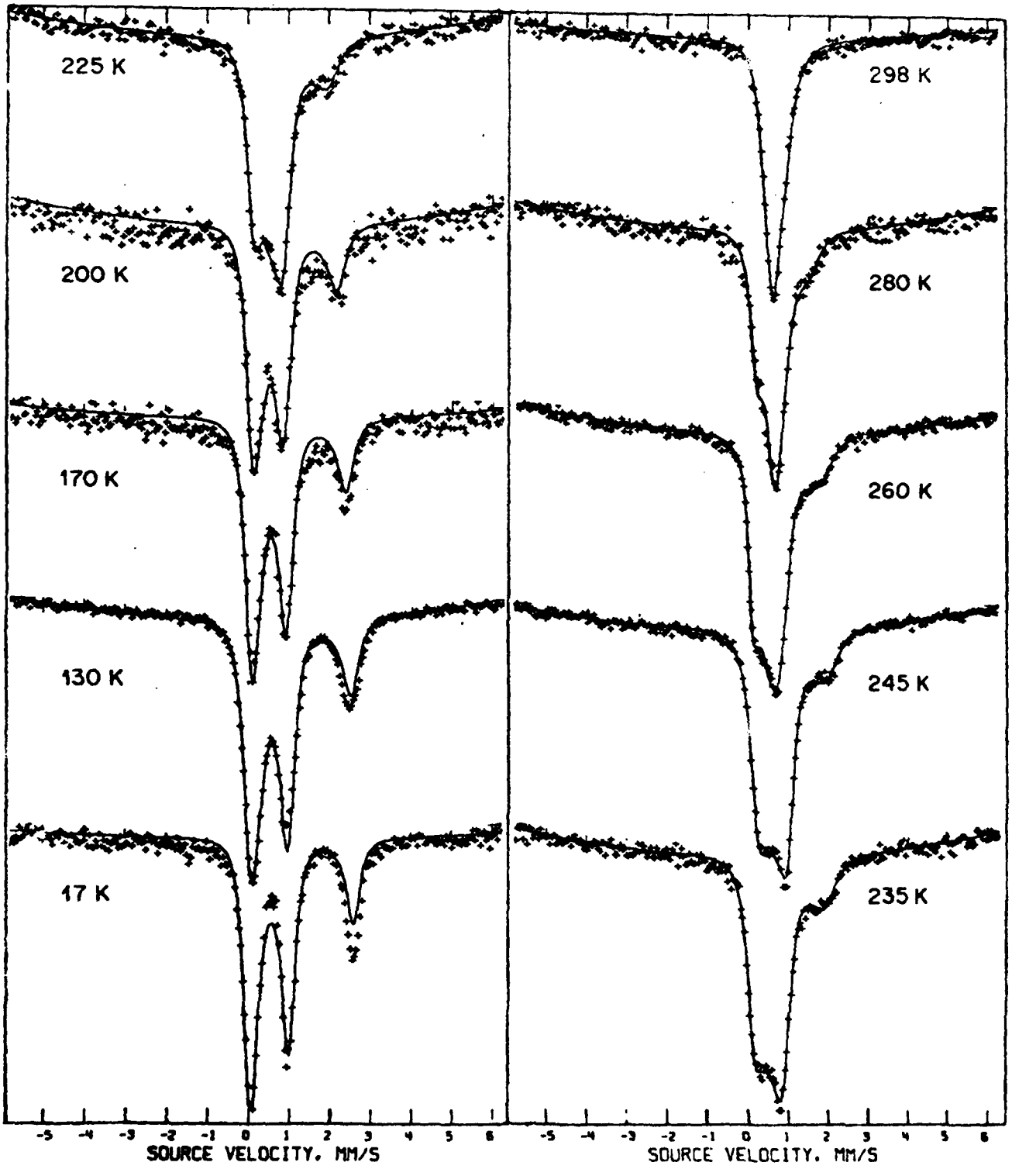
225 K
200 K
170 K
130 K
17 K
298 K
280 K
260 K
245 K
235 K
-5 -4 -3 -2 -1 0 1 2 3 4 5 6
SOURCE VELOCITY, MM/S
-5 -4 -3 -2 -1 0 1 2 3 4 5 6
SOURCE VELOCITY, MM/S

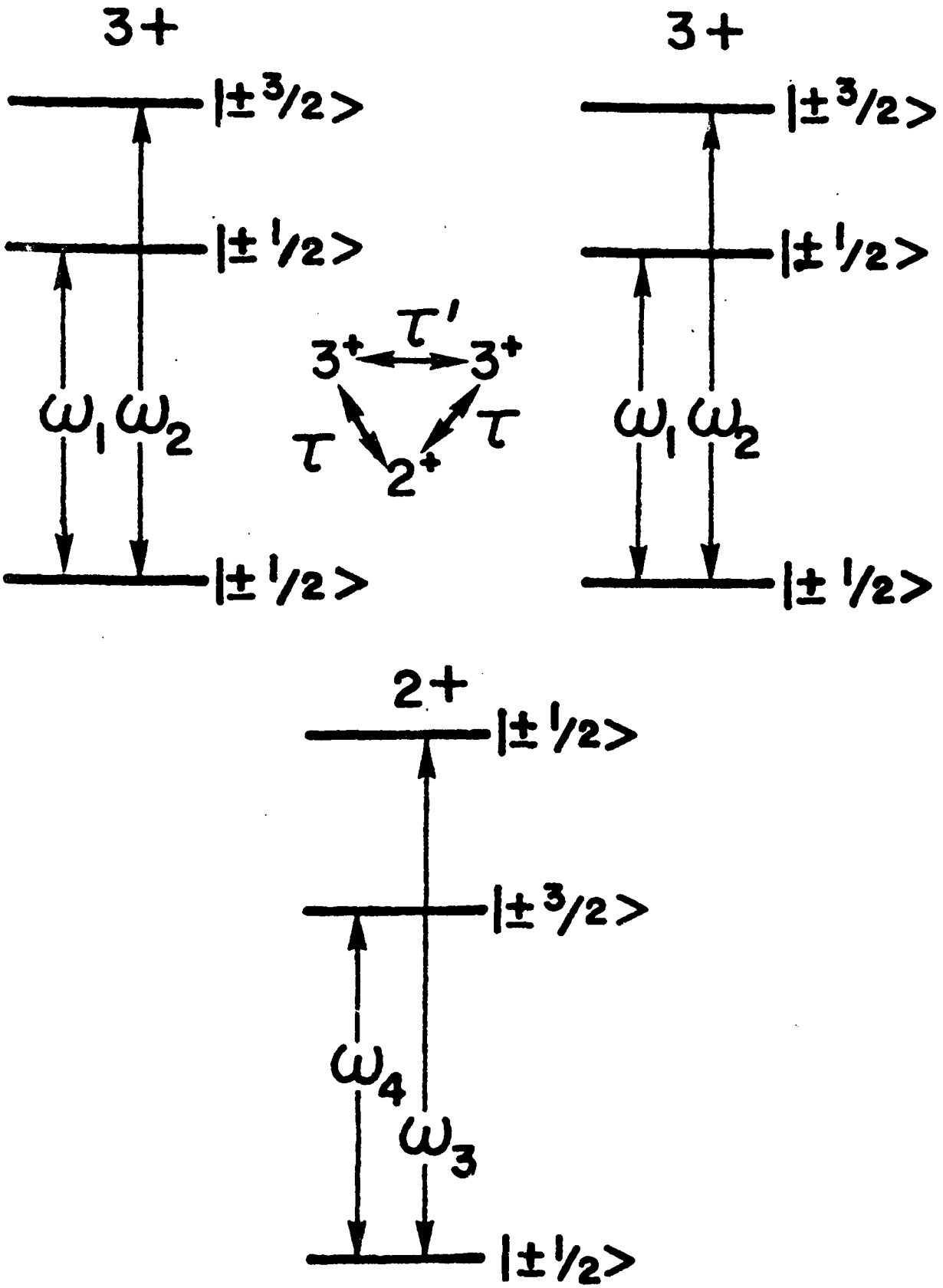
3+
|±3/2>
|±1/2>
ω1 ω2
|±1/2>
τ'
3+ 3+
τ τ
2+
3+
|±3/2>
|±1/2>
ω1 ω2
|±1/2>
2+
|±1/2>
|±3/2>
ω4
ω3
|±1/2>

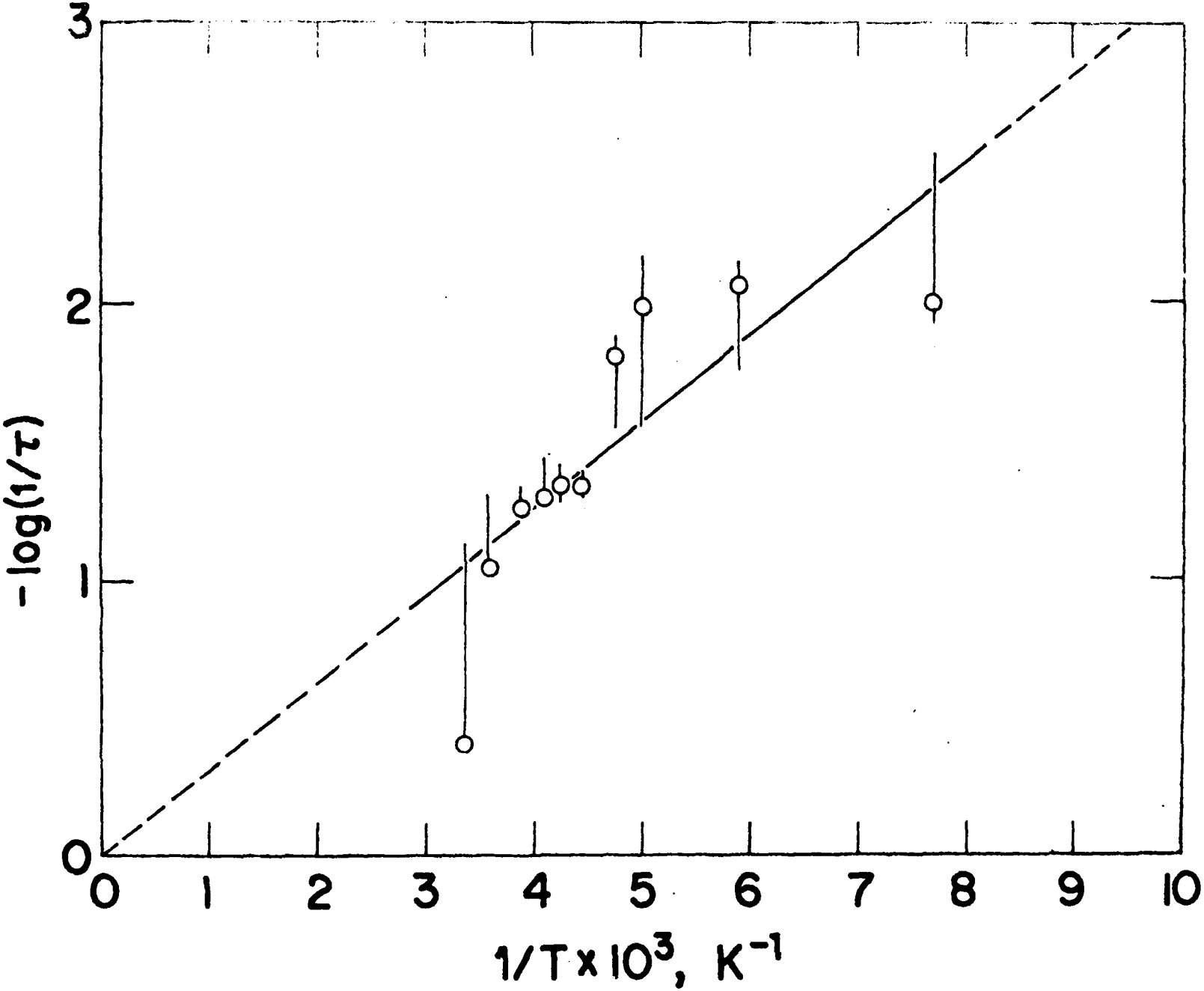
3
2
1
0
-log(1/τ)
0
1
2
3
4
5
6
7
8
9
10
1/T x 10³, K⁻¹

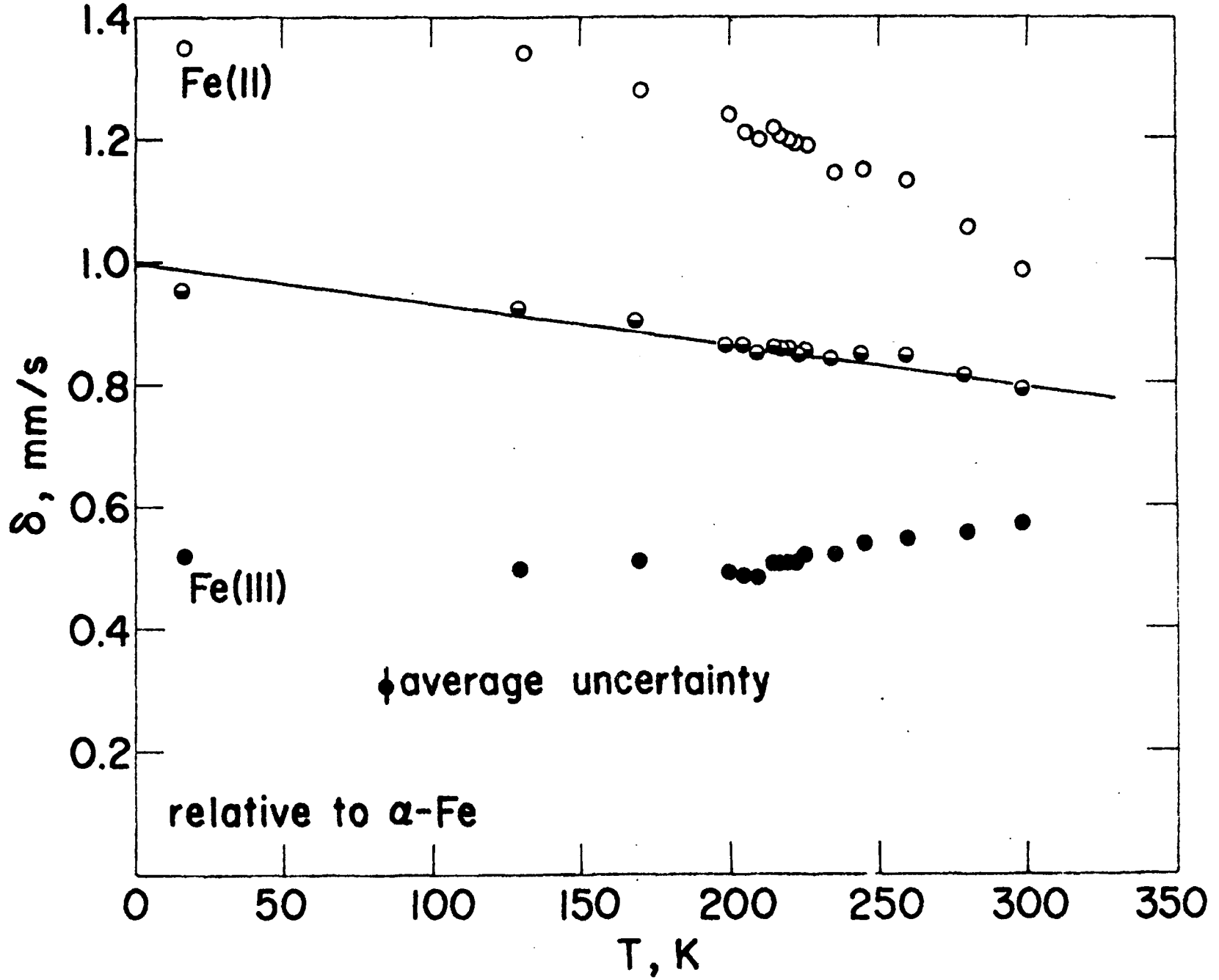
1.4
1.2
1.0
0.8
0.6
0.4
0.2
δ, mm/s
Fe(II)
Fe(III)
average uncertainty
relative to α-Fe
0
50
100
150
200
250
300
350
T, K

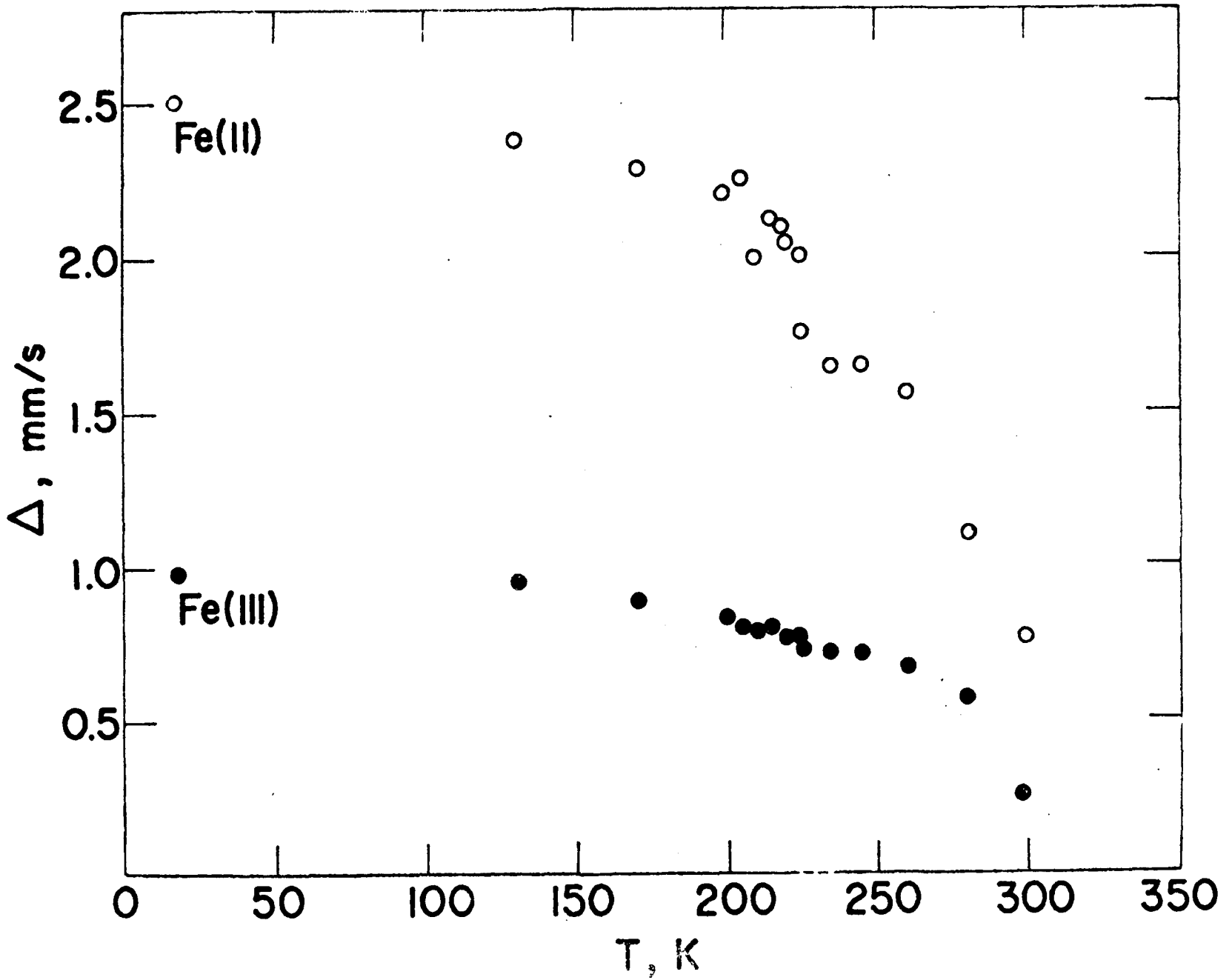
2.5
2.0
1.5
1.0
0.5
Δ, mm/s
Fe(II)
Fe(III)
0
50
100
150
200
250
300
350
T, K

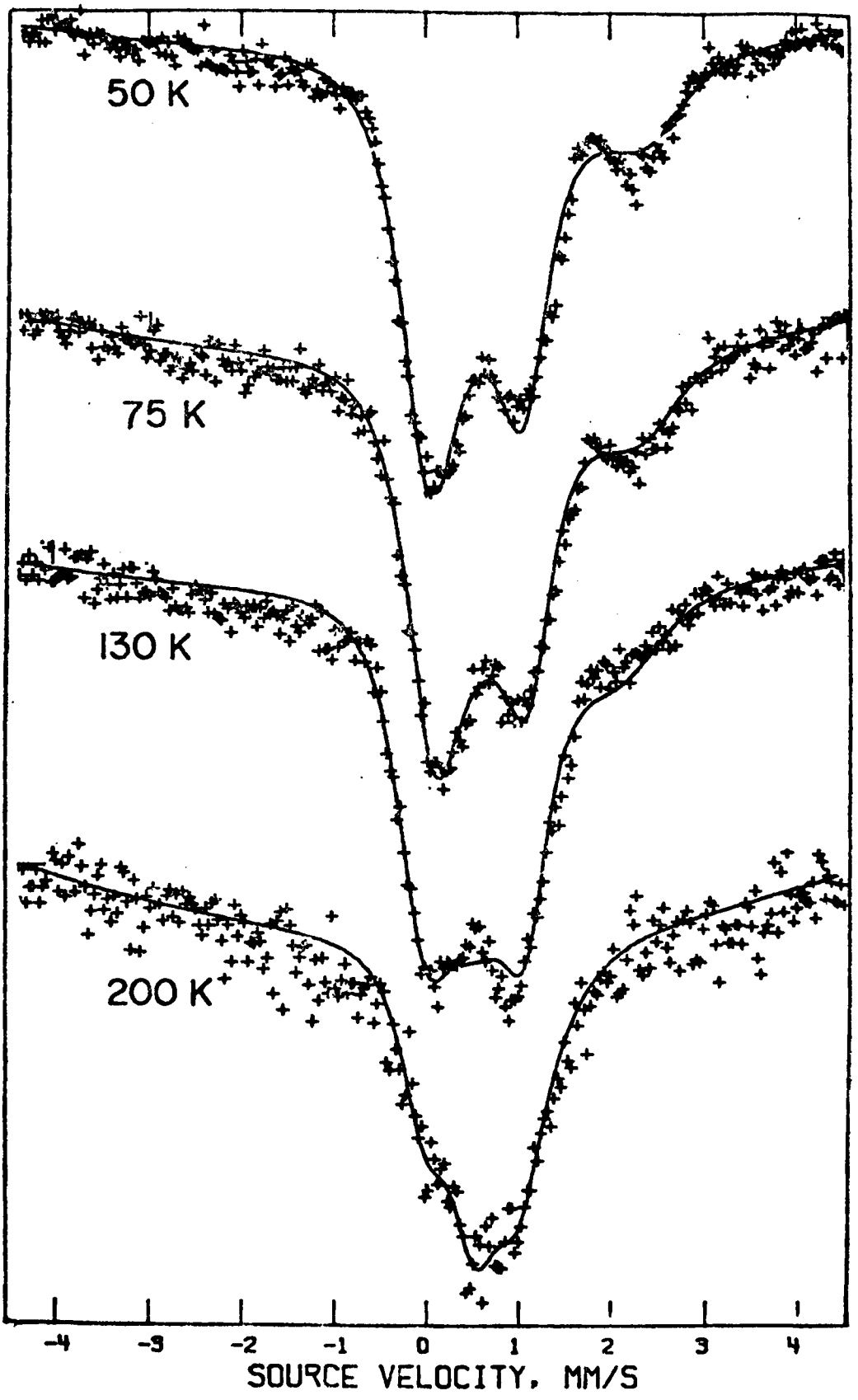
50 K
75 K
130 K
200 K
-4
-3
-2
-1
0
1
2
3
4
SOURCE VELOCITY, MM/S

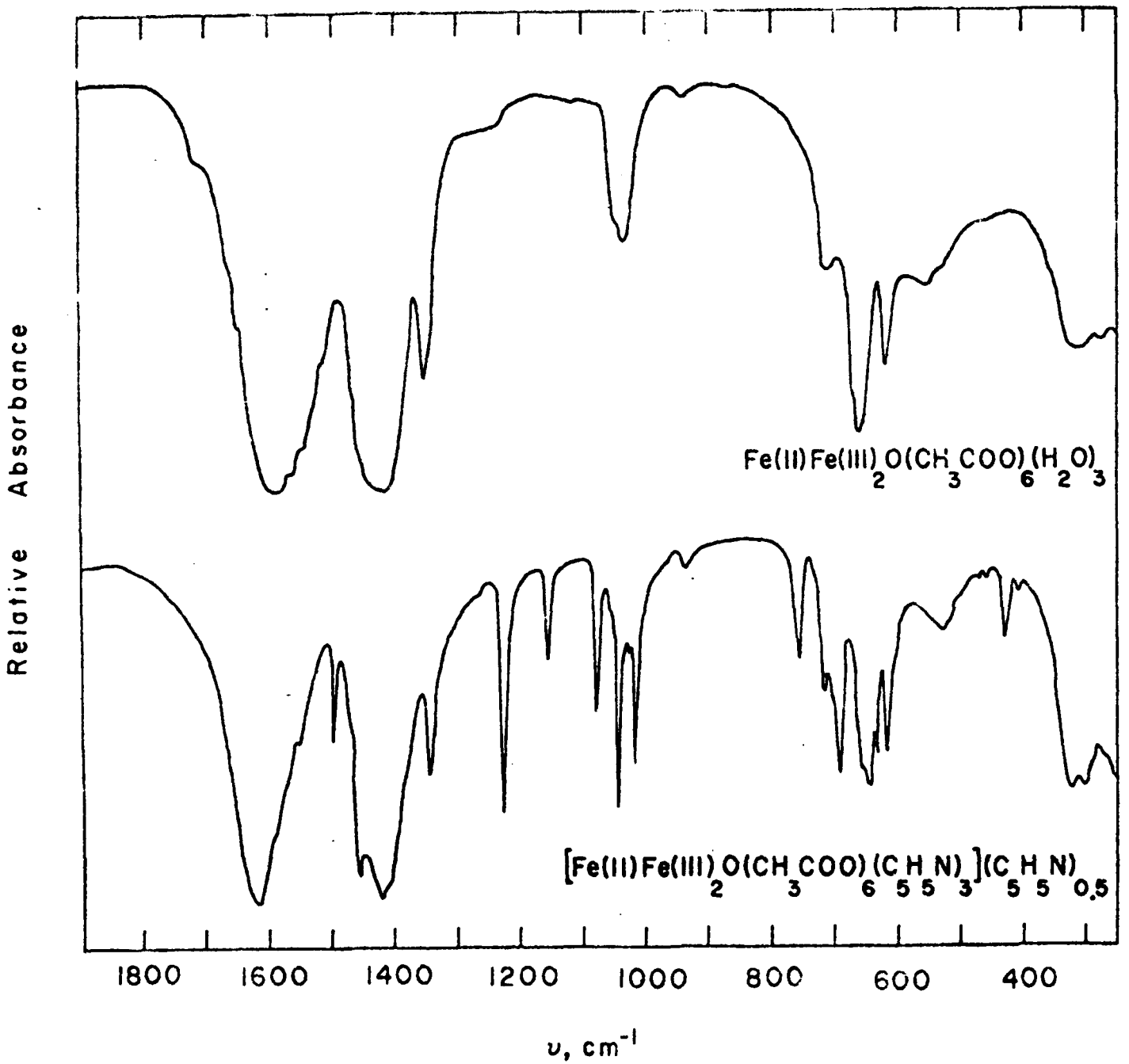
Relative Absorbance
Fe(II)Fe(III)2O(CH3COO)6(H2O)3
[Fe(II)Fe(III)2O(CH3COO)6(C5H5N)3](C5H5N)0.5
1800
1600
1400
1200
1000
800
600
400
υ, cm-1

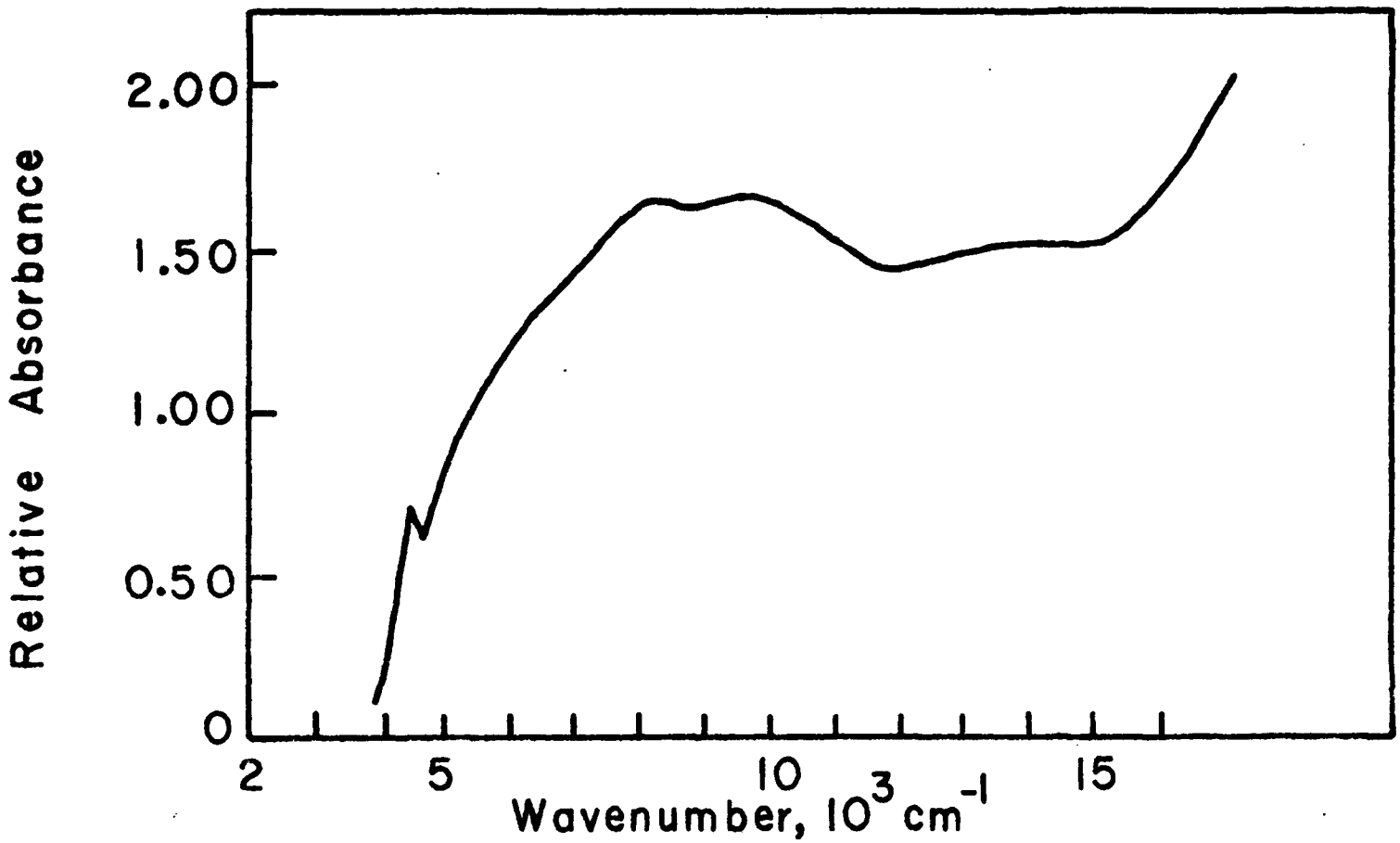
Relative Absorbance
2.00
1.50
1.00
0.50
0
2
5
10
15
Wavenumber, 10^3 cm^{-1}

TECHNICAL REPORT DISTRIBUTION LIST, 053

	No. Copies
Dr. R. N. Grimes Department of Chemistry University of Virginia Charlottesville, Virginia 22901	1
Dr. M. F. Hawthorne Department of Chemistry University of California Los Angeles, California 90024	1
Dr. W. B. Fox Chemistry Division Naval Research Laboratory Code 6130 Washington, D.C. 20375	1
Dr. J. Adcock Department of Chemistry University of Tennessee Knoxville, Tennessee 37916	1
Dr. A. Cowley Department of Chemistry University of Texas Austin, Texas 78712	1
Dr. W. Hatfield Department of Chemistry University of North Carolina Chapel Hill, North Carolina 27514	1
Dr. D. Seyferth Department of Chemistry Massachusetts Institute of Technology Cambridge, Massachusetts 02139	1
Professor Ralph Rudolph Department of Chemistry University of Michigan Ann Arbor, Michigan 48109	1
Professor H. Abrahamson Department of Chemistry University of Oklahoma Norman, Oklahoma 73019	1
Professor M. Newcomb Texas A&M University Department of Chemistry College Station, Texas 77843	1

	No. Copies
Dr. M. H. Chisholm Department of Chemistry Indiana University Bloomington, Indiana 47401	1
Dr. B. Foxman Department of Chemistry Brandeis University Waltham, Massachusetts 02154	1
Dr. T. Marks Department of Chemistry Northwestern University Evanston, Illinois 60201	1
Dr. G. Geoffrey Department of Chemistry Pennsylvania State University University Park, Pennsylvania 16802	1
Dr. J. Zuckerman Department of Chemistry University of Oklahoma Norman, Oklahoma 73019	1
Professor O. T. Beachley Department of Chemistry State University of New York Buffalo, New York 14214	1
Professor P. S. Skell Department of Chemistry The Pennsylvania State University University Park, Pennsylvania 16802	1
Professor K. M. Nicholas Department of Chemistry Boston College Chestnut Hill, Massachusetts 02167	1
Professor R. Neilson Department of Chemistry Texas Christian University Fort Worth, Texas 76129	1
Professor Richard Eisenberg Department of Chemistry University of Rochester Rochester, New York 14627	1

TECHNICAL REPORT DISTRIBUTION LIST, GEN

	No. Copies
Office of Naval Research Attn: Code 472 800 North Quincy Street Arlington, Virginia 22217	2
ONR Branch Office Attn: Dr. George Sandoz 536 S. Clark Street Chicago, Illinois 60605	1
ONR Area Office Attn: Scientific Dept. 715 Broadway New York, New York 10003	1
ONR Western Regional Office 1030 East Green Street Pasadena, California 91106	1
ONR Eastern/Central Regional Office Attn: Dr. L.H. Peebles Building 114, Section D 666 Summer Street Boston, Massachusetts 02210	1
Director, Naval Research Laboratory Attn: Code 6100 Washington, D.C. 20390	1
The Assistant Secretary of the Navy (RE&S) Department of the Navy Room 4E736, Pentagon Washington, D.C. 20350	1
Commander, Naval Air Systems Command Attn: Code 310C (H. Rosenwasser) Department of the Navy Washington, D.C. 20360	1
Defense Technical Information Center Building 5, Cameron Station Alexandria, Virginia 22314	12
Dr. Fred Saalfeld Chemistry Division, Code 6100 Naval Research Laboratory Washington, D.C. 20375	1
Dr. Rudolph J. Marcus Office of Naval Research Scientific Liaison Group American Embassy APO San Francisco 96503	1
U.S. Army Research Office Attn: CRD-AA-IP P.O. Box 1211 Research Triangle Park, N.C. 27709	1
Naval Ocean Systems Center Attn: Mr. Joe McCartney San Diego, California 92152	1
Naval Weapons Center Attn: Dr. A. B. Amster, Chemistry Division China Lake, California 93555	1
Naval Civil Engineering Laboratory Attn: Dr. R. W. Drisko Port Hueneme, California 93401	1
Department of Physics & Chemistry Naval Postgraduate School Monterey, California 93940	1
Dr. A. L. Slafkosky Scientific Advisor Commandant of the Marine Corps (Code RD-1) Washington, D.C. 20380	1
Office of Naval Research Attn: Dr. Richard S. Miller 800 N. Quincy Street Arlington, Virginia 22217	1
Naval Ship Research and Development Center Attn: Dr. G. Bosmajian, Applied Chemistry Division Annapolis, Maryland 21401	1
Naval Ocean Systems Center Attn: Dr. S. Yamamoto, Marine Sciences Division San Diego, California 91232	1
Mr. John Boyle Materials Branch Naval Ship Engineering Center Philadelphia, Pennsylvania 19112	1
Mr. James Kelley DTNSRDC Code 2803 Annapolis, Maryland 21402	1